New Routes to η^1- and ($\eta^3 \leftrightarrow \eta^5$)-Indenylpalladium Complexes: Synthesis, Characterization, and Reactivities

Christine Sui-Seng,[†] Gary D. Enright,[‡] and Davit Zargarian*,[†]

Département de chimie, Université de Montréal, Québec, Canada H3C 3J7, and Steacie Institute for Molecular Sciences, National Research Council, Ottawa, Ontario, Canada K1A 0R6

Received October 22, 2003

The dimer {(η^3-Ind)Pd(μ-Cl)}$_2$ (**6**) reacts with *t*-BuNC to give the dimeric species {(η^1-Ind)(*t*-BuNC)Pd(μ-Cl)}$_2$ (**10**), whereas reaction with PR_3 gives the complexes (η-Ind)Pd(PR_3)Cl (R = Ph (**4**), Cy (**7**), Me (**8**), OMe (**9**)). Complexes **4** and (1-Me-Ind)Pd(PPh_3)Cl (**5**) can also be prepared by reacting $(PhCN)_2PdCl_2$ with LiInd and PPh_3. The structural characterization of complexes **4**−**7**, **9**, and **10** by ^{1}H and ^{13}C NMR spectroscopy and single-crystal X-ray diffraction studies has allowed an analysis of the indenyl ligand's mode of coordination, both in the solid-state and in solution. Compounds **4**, **6**, and **7** react with $PhSiH_3$ in the absence of cocatalysts, whereas reaction with ethylene requires the presence of excess MAO to give polyethylene.

Introduction

In comparison to their Cp analogues, some indenyl complexes of transition metals possess enhanced reactivities in catalysis and in various stoichiometric reactions, notably ligand substitution. This characteristic has been attributed to the relative ease with which metals can slip reversibly across the indenyl ligand's five-membered ring, thus forming a reactive η^3-indenyl tautomer that has both benzenoid resonance stabilization and an accessible coordination site on the metal. Various manifestations of this so-called "indenyl effect",[1] including superior catalytic activities,[2] have been observed for many indenyl complexes, in particular those of group 6−9 metals.[3] In contrast, the chemistry of group 10 metal indenyl complexes is at an early phase of its development.[4]

Our group has studied the chemistry of the complexes IndNi(L)(X) (Ind = indenyl and its substituted derivates),[5] some of which can act as precatalysts in the oligo- and polymerization of alkenes,[6] alkynes,[7] and $PhSiH_3$[8] and in the hydrosilylation of alkenes and ketones.[9] Our interest in the structures and catalytic activities of the IndNi complexes prompted us to explore the chemistry of analogous Pd compounds in order to elucidate the influence of the metal center on the chemistry of these compounds. Relatively little is known about the reactivities of IndPd complexes, but the preparation and characterization of the following compounds have been reported: {(η^3-Ind)Pd(μ-Cl)}$_2$,[10] {(μ-η^3-Ind)Pd(CNR)}$_2$ (R = *t*-Bu, 2,6-$(CH_3)_2C_6H_3$, 2,4,6-$(CH_3)_3C_6H_2$, 2,4,6-(*t*-Bu)$_3C_6H_2$),[11] (η^3-Ind)Pd(PMe_3)($CH(SiMe_3)_2$),[12] and [(η^3-Ind)Pd(LL)]$^+$[13] (LL = bipy, tmeda). In addition, a preliminary communication has appeared on the preparation of a series of Ind derivates from the reaction of cyclopropene and $(PhCN)_2PdCl_2$.[14]

[†] Université de Montréal.
[‡] National Research Council.

(1) (a) Rerek, M. E.; Ji, L.-N.; Basolo, F. *J. Chem. Soc., Chem. Commun.* **1983**, 1208. (b) Ji, L.-N.; Rerek, M. E.; Basolo, F. *Organometallics* **1984**, *3*, 740. (c) Casey, C. P.; O'Connor, J. M. *Organometallics* **1985**, *4*, 384. (d) O'Connor, J. M.; Casey, C. P. *Chem. Rev.* **1987**, *87*, 307.

(2) (a) Frankom, T. M.; Green, J. C.; Nagy, A.; Kakkar, A. K.; Marder, T. B. *Organometallics* **1993**, *12*, 3688. (b) Gamasa, M. P.; Gimeno, J.; Gonzalez-Bernado, C.; Martin-Vaca, B. M.; Monti, D.; Basseti, M. *Organometallics* **1995**, *15*, 302.

(3) Reactivity differences have also been noted between the Cp/Ind complexes of early transition metals, but since these complexes are generally electronically unsaturated, their reactivity differences are less likely to be related to the hapticity of the ligands and more likely influenced by steric and symmetry factors.

(4) For a recent review on the chemistry of group 10 metal indenyl complexes see: Zargarian, D. *Coord. Chem. Rev.* **2002**, *233*−*234*, 157.

(5) (a) Huber, T. A.; Bélanger-Gariépy, F.; Zargarian, D. *Organometallics* **1995**, *14*, 4997. (b) Bayrakdarian, M.; Davis, M. J.; Dion, S.; Dubuc, I.; Bélanger-Gariépy, F.; Zargarian, D. *Can. J. Chem.* **1996**, *74*, 2115. (c) Huber, T. A.; Bayrakdarian, M.; Dion, S.; Dubuc, I.; Bélanger-Gariépy, F.; Zargarian, D. *Organometallics* **1997**, *16*, 5811. (d) Groux, L. F.; Bélanger-Gariépy, F.; Zargarian, D.; Vollmerhaus, R. *Organometallics* **2000**, *19*, 1507. (e) Fontaine, F.-G.; Dubois, M.-A.; Zargarian, D. *Organometallics* **2001**, *20*, 5156.

(6) (a) Vollmerhaus, R.; Bélanger-Gariépy, F.; Zargarian, D. *Organometallics* **1997**, *16*, 4762. (b) Dubois, M.-A.; Wang, R.; Zargarian, D.; Tian, J.; Vollmerhaus, R.; Li, Z.; Collins, S. *Organometallics* **2001**, *20*, 663. (c) Groux, L. F.; Zargarian, D. *Organometallics* **2001**, *20*, 3811. (d) Groux, L. F.; Zargarian, D.; Simon, L. C.; Soares, J. B. P. *J. Mol. Catal. A* **2003**, *193*(1−2), 51. (e) Groux, L. F.; Zargarian, D. *Organometallics* **2003**, *22*, 3124. (f) Groux, L. F.; Zargarian, D. *Organometallics* **2003**, *22*, ASAP.

(7) (a) Wang, R.; Bélanger-Gariépy, F.; Zargarian, D. *Organometallics* **1999**, *18*, 5548. (b) Wang, R.; Groux, L. F.; Zargarian, D. *Organometallics* **2002**, *21*, 5531. (c) Wang, R.; Groux, L. F.; Zargarian, D. *J. Organomet. Chem* **2002**, *660*(1), 98. (d) Rivera, E.; Wang, R.; Zhu, X. X.; Zargarian, D.; Giasson, R. *J. Mol. Catal. A* **2003**, *204*−*205*, 325.

(8) (a) Fontaine, F.-G.; Kadkhodazadeh, T.; Zargarian, D. *J. Chem. Soc., Chem. Commun.* **1998**, 1253−1254. (b) Fontaine, F.-G.; Zargarian, D. *Organometallics* **2002**, *21*, 401.

(9) Fontaine, F.-G.; Nguyen, R.-V.; Zargarian, D. *Can. J. Chem.* **2003**, *81*, 1299.

(10) (a) Nakasuji, K.; Yamaguchi, M.; Murata, I.; Tatsumi, K.; Natamura, A. *Organometallics* **1984**, *3*, 1257. (b) Samuel, E.; Bigorgne, M. *J. Organomet. Chem.* **1969**, *19*, 9.

(11) Tanase, T.; Nomura, T.; Fukushina, T.; Yamamoto, Y.; Kobayashi, K. *Inorg. Chem.* **1993**, *32*, 4578.

(12) (a) Alias, F. M.; Belderrain, T. R.; Paneque, M.; Poveda, M. L.; Carmona, E. *Organometallics* **1998**, *17*, 5620. (b) Alias, F. M.; Belderrain, T. R.; Carmona, E.; Graiff, C.; Paneque, M.; Poveda, M. L. *J. Organomet. Chem.* **1999**, *577*, 316.

(13) (a) Vicente, J.; Abad, J.-A.; Bergs, R.; Jones, P. G.; De Arellano, M. C. R. *Organometallics* **1996**, *15*, 1422. (b) Vicente, J.; Abad, J.-A.; Bergs, R.; De Arellano, M. C. R.; Martinez-Vivente, E.; Jones, P. G. *Organometallics* **2000**, *19*, 5597.

10.1021/om034253n CCC: $27.50
Publication on Web 02/10/2004

Scheme 1

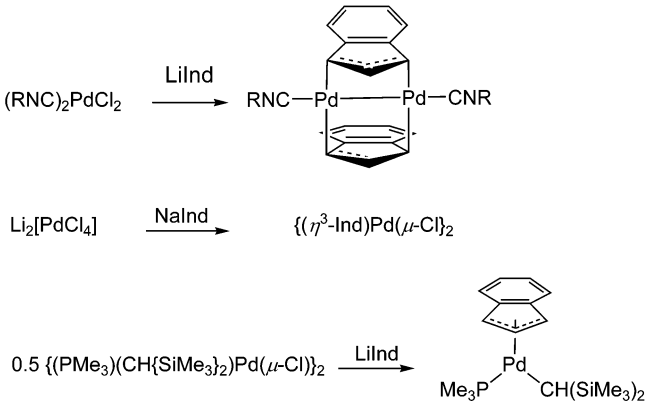

Scheme 2

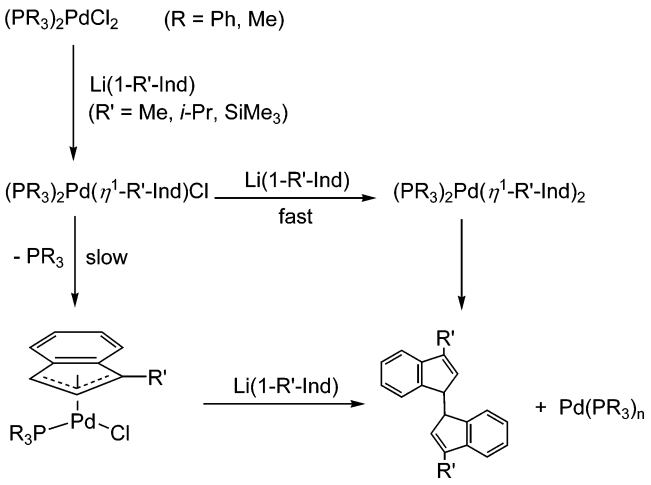

Herein we report two different synthetic routes to the complexes (η-Ind)Pd(PR_3)Cl (R= Ph, Cy, Me, OMe) and compare their structures and reactivities to those of their analogous Ni complexes. The preparation of the dimeric complex {(η^1-Ind)(*t*-BuNC))Pd(μ-Cl)}$_2$ from the precursor {(η^3-Ind)Pd(μ-Cl)}$_2$ and the solid-state structures of these dimeric species will also be described.

Results and Discussion

Synthesis. The main synthetic pathway to known IndPd compounds involves the metathetic reactions of MInd (M = Li, Na) with various L_nPdCl_m precursors (Scheme 1).[10−12] However, when we applied this methodology for the synthesis of the complexes IndPd(PR_3)Cl from the precursors $(PR_3)_2PdCl_2$ (R = Ph, Me), we obtained the homocoupling products 1,1′-biindene and Pd(PR_3)$_n$ (Scheme 2). A similar observation has been made during the syntheses of the analogous IndNi(PR_3)Cl complexes.[5a] These side reactions may be attributed to the sequence of steps depicted in Scheme 2: reaction of Ind$^-$ with the precursors gives the initial intermediate (η^1-Ind)M$(PR_3)_2$Cl; conversion of the latter to the desired (η-Ind)M(PR_3)Cl is hampered by the slow dissociation of one of the phosphine ligands;[15] this brings about the competitive addition of a second equivalent of Ind$^-$ to give (η^1-Ind)$_2$M$(PR_3)_2$, which produces 1,1′-biindene and M$^0(PR_3)_n$, presumably by reductive elimination.[16]

Scheme 3

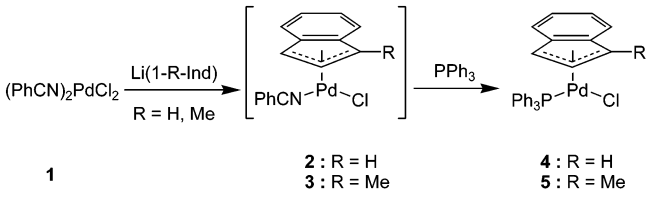

In an attempt to circumvent the above-discussed homocoupling side reaction, we studied the use of alkyl-substituted Ind precursors Li(1-R-Ind) (R = Me, *i*-Pr, $SiMe_3$), a strategy that was successful in suppressing the coupling side reaction in the case of Ni precursors.[5c] Interestingly, however, this approach had no effect on the course of the Pd reactions, implying that the Pd precursors are more effective for the coupling reaction.[17]

We surmised that the use of Pd precursors bearing more labile auxiliary ligands would accelerate ligand dissociation from the putative intermediate (η^1-Ind)PdL_2Cl (Scheme 2), thereby favoring the formation of the target complexes. Indeed, reacting $(PhCN)_2PdCl_2$ (**1**) with Li(1-R-Ind) (R = H, Me) appeared to give the target complexes IndPd(NCPh)Cl, as indicated by a color change from yellow to dark brown; the isolation of the new products was hampered, however, by a gradual decomposition that occurred even at −78 °C to give an insoluble black solid. To circumvent this decomposition, we added ca. 0.6 equiv of PPh_3 to the reaction mixture following the addition of Li(1-R-Ind) in order to convert the presumably thermally unstable IndPd(NCPh)Cl to the phosphine adduct (Scheme 3). This approach led to the isolation of (1-R-Ind)Pd(PPh_3)Cl (R = H (**4**), Me (**5**)) as brown-red powders in moderate yields (36% on the basis of $(PhCN)_2PdCl_2$, 60% on the basis of PPh_3). It is noteworthy that reacting **1** with a mixture of LiInd and PPh_3 at −78 °C, or adding LiInd to a mixture of **1** and PPh_3 at low temperature, produced 1,1′-biindene and only a small amount of the target complexes **4** and **5**, giving mainly $(PPh_3)_2PdCl_2$ and Pd(0).

The low yields obtained from the metathetic reactions outlined above prompted us to explore alternative routes not involving anionic sources of Ind in order to minimize the homocoupling side reaction. Indeed, Boudjouk and Lin have reported that 1-$SiMe_3$-Ind can be an effective source for the preparation of the polymeric species {(η^3-Ind)Pd(μ-Cl)}$_n$ (Scheme 4).[18] The latter seemed like a promising precursor to the complexes (η-Ind)Pd(L)Cl. This approach was attempted and proved successful, as described below.

(14) Fiato, R. A.; Mushak, P.; Battiste, M. A. *J. Chem. Soc., Chem. Commun.* **1975**, 869.

(15) Consistent with this proposal, this side reaction is most prevalent with the Ni precursors containing the weakly labile ligand PMe_3.

(16) Different metal-containing side products are generated in this side reaction depending on the metallic precursors used. For example, $(PPh_3)_2Ni^{II}Cl_2$ generates $(PPh_3)_3Ni^{I}Cl$, which is thought to arise from the conproportionation of the Ni^{II} precursor and the $(PPh_3)_nNi^0$ species generated in the coupling reaction. On the other hand, reaction of the analogous $(PMe_3)_2NiCl_2$ gives only $Ni(PMe_3)_4$, which can be detected by its characteristic ^{31}P signal at − 22 ppm (Tolman, C. A. *J. Am. Chem. Soc.* **1970**, *92*, 2956). For the palladium precursor $(PPh_3)_2PdCl_2$, only the species $Pd(PPh_3)_n$ (n = 3, 4) has been detected by $^{31}P\{^1H\}$ NMR (singlet at +24 ppm).

(17) We have noted that the independently prepared (η-Ind)Pd(PR_3)Cl species react much more readily than their Ni counterparts with IndLi to give 1,1′-biindene; this might explain why the metathetic routes involving Ind anions are particularly ineffective for the synthesis of indenyl−Pd complexes.

(18) Lin, S.; Boudjouk, P. *J. Chin. Chem. Soc.* **1989**, *36*, 35.

Scheme 4

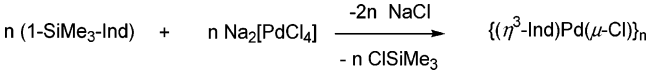

Scheme 5

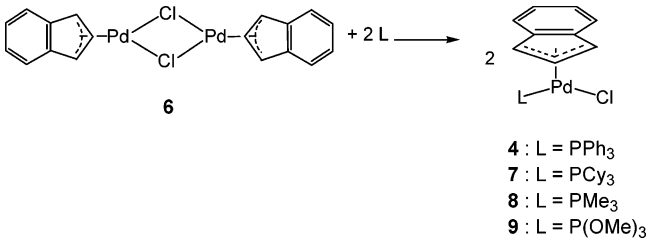

Reacting 8.3 mmol of 1-$SiMe_3$-Ind with 7.2 mmol of $Na_2[PdCl_4]$ in ethanol gave a brown mixture from which a brown solid precipitated gradually. Filtration and successive washing of the collected solid with distilled water, Et_2O, and ethanol gave a material whose physical appearance matched that of the compound $\{(\eta^3\text{-Ind})Pd(\mu\text{-Cl})\}_n$, reported by Boudjouk and Lin.[18] Interestingly, however, the NMR data for this product were different from those reported by Boudjouk and Lin but exactly similar to the data reported by Murata's group for the dimer $\{(\eta^3\text{-Ind})Pd(\mu\text{-Cl})\}_2$ (**6**).[10a] To establish the identity of this compound unequivocally, we undertook an X-ray diffraction study that confirmed the dimeric structure of the product of our synthesis (vide infra). The factors responsible for the preferred formation in our syntheses of the dimer, as opposed to the polymeric species proposed by Boudjouk and Lin, are not known. Nevertheless, in our hands Boudjouk's procedure gives access to 80−90% yields of complex **6**, which has served as a versatile precursor for the preparation of other IndPd complexes, as outlined below.

The monomeric phosphine adducts $(\eta\text{-Ind})Pd(PR_3)Cl$ (R = Ph (**4**), Cy (**7**), Me (**8**), OMe (**9**)) were obtained by reacting the dimeric product **6** with PR_3 (Scheme 5); these complexes have been isolated as orange-red solids in ca. 70−90% yields. On the other hand, a different reactivity was observed when **6** was reacted with CO and *t*-BuNC. Thus, reaction with CO resulted in a color change from brown to red, but this change was maintained only as long as the solution was saturated with CO. The ^1H NMR spectrum of the mixture (with CO present in the head gas) showed that the signals due to **6** had been replaced by a series of broad peaks, while the $^{13}C\{^1H\}$ NMR spectrum displayed no signals at all, implying an exchange process. Curiously, the IR spectrum did not show any absorption in the ν(CO) region. All attempts at isolating the new species were unsuccessful, as evaporation of the solvent or addition of hexane to precipitate the product resulted in the regeneration of the starting material. We conclude, therefore, that the putative CO adduct is in equilibrium with **6**.

In contrast, *t*-BuNC converted **6** to the dimeric derivative $\{(\eta^1\text{-Ind})(t\text{-BuNC})Pd(\mu\text{-Cl})\}_2$ (**10**; Scheme 6), which could be isolated in 57% yield. Complex **10** is the first example of an isolated and fully characterized Pd^{II} complex featuring an η^1-Ind moiety, but Poveda and coworkers have reported the in situ generation and spectroscopic characterization of a monomeric $(\eta^1\text{-Ind})Pd^{II}$ complex (Scheme 7).[12a] The conversion of **6** to the complexes **4** and **7**−**10** is analogous to a ligand displacement reaction and likely proceeds by the initial coordination of the incoming ligand (associative mechanism); it is interesting to note, however, that phosphine ligands displace the bridging Cl, whereas *t*-BuNC causes a change in the hapticity of Ind.

Scheme 6

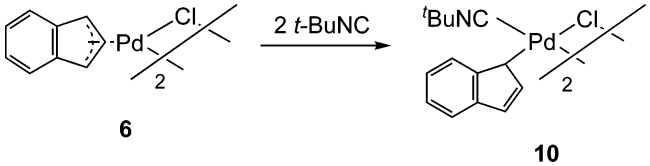

Scheme 7

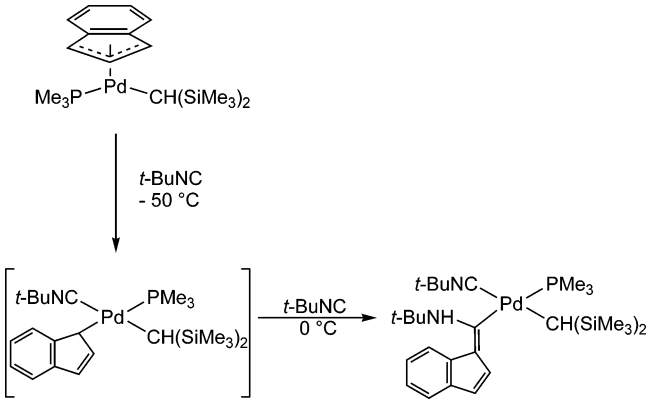

Compounds **4**−**10** are thermally stable and can be handled in air for a few hours (both in the solid and in solution) without appreciable decomposition. The identities of these complexes were deduced from their NMR spectra and confirmed by the results of elemental analyses and single-crystal X-ray diffraction studies. These studies have provided valuable information on the structural features of this family of complexes, as described in the following section.

Spectroscopic Characterization. A singlet resonance is observed in the $^{31}P\{^1H\}$ NMR spectra of the complexes **4**, **5**, and **7**−**9**, similar to those of the analogous Ni compounds; in the case of **4**, **5**, and **8**, the ^{31}P chemical shifts are close to the corresponding signals of their Ni homologues (Table 1). The ^1H NMR and $^{13}C\{^1H\}$ NMR spectra of these compounds were also quite similar to those of the corresponding Ni compounds. Reliable peak assignments were made by means of inverse-gated decoupling, COSY, and HMQC experiments; the results of these detailed studies have proven particularly informative for the coordination mode of the Ind ligand in these compounds. For instance, the ^{13}C NMR spectra of Ind complexes can help identify the type of M−Ind interactions present in solution following an empirical protocol described by Baker[19] and Marder.[20] According to this protocol, the magnitude of the parameter $\Delta\delta_{av}(^{13}C) = \delta_{av}$(C3a/C7a of M-Ind) − δ_{av}(C3a/C7a of Na^+Ind^-) (ca. 130.7 ppm) reflects the solution hapticity of the Ind ligand in a given complex; thus, the solution hapticity is thought to be closer to η^5 when $\Delta\delta_{av}(C) \ll 0$ (e.g., $\Delta\delta_{av}$(C) for Ind_2Fe is ca. − 42 ppm),[20] closer to η^3 when $\Delta\delta_{av}(C) \gg 0$ (e.g., $\Delta\delta_{av}$(C) for (Ind)Ir-

(19) Baker, R. T.; Tulip, T. H. *Organometallics* **1986**, *5*, 839.
(20) Westcott, S. A.; Kakkar. A. K.; Stringer, G.; Taylor, N. J.; Marder, T. B. *J. Organomet. Chem.* **1990**, *394*, 777.

Table 1. Electrochemical and NMR Data for Complexes 4−9 and Analogous Nickel Complexes[a]

compd	$^{31}P\{^1H\}$ (δ, ppm)	H_1/H_3 (δ, ppm) H_3	C_1/C_3 (δ, ppm)	$\Delta\delta_{av}$ (ppm)	E_{red1}[e] (V)	E_{red2}[e] (V)
(Ind)Pd(PPh_3)Cl (**4**)	27.98	6.51/4.57	97.2/79.9	6.7	−0.94	−1.41
(Ind)Ni(PPh_3)Cl (**11**)	28.20	5.91/3.33[b]	90.2/69.71[b]	−2	−0.64	
(1-Me-Ind)Pd(PPh_3)Cl (**5**)	30.03	−/4.28	113.3/76.5	8.5	−1.03	−1.48
(1-Me-Ind)Ni(PPh_3)Cl (**12**)	31.10	−/3.37	103.4/67.2[c]	−2.0	−0.75	−1.05
(Ind)Pd(PCy_3)Cl (**7**)	49.04	6.21/5.11	94.3/ 70.9	8.5	−1.07	−1.64
(1-Me-Ind)Ni(PCy_3)Cl	37.17	−/4.11	97.10/55.42	−1.0		
(Ind)Pd(PMe_3)Cl (**8**)	−7.56	6.42/5.26	97.0/ 70.2	6.6	−1.24	−1.24
(1-Me-Ind)Ni(PMe_3)Cl	−10.61	−/3.58	101.29/59.53	−2.0		
(Ind)Pd($P(OMe)_3$Cl (**9**)	131.21[d]	6.49/5.69[d]	99.4/ 73.2[d]	6.3[d]		

[a] Unless otherwise indicated, all spectroscopic data were collected at room temperature in C_6D_6. [b] At 233 K, in toluene-d_8. [c] In acetone-d_6. [d] In $CDCl_3$. [e] In CH_3CN.

Chart 1

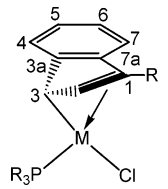

(η^1, η^2)

(PMe_3)$_3$ is ca. +28 ppm),[21] and intermediate when $\Delta\delta_{av}(C) \approx 0$ (e.g., $\Delta\delta_{av}(C)$ for $(Ind)_2Ni$[22] is ca. +5 ppm).[20] The $\Delta\delta_{av}(C)$ values for our complexes are ca. +6.5 ppm for **4**, **6**, **8**, and **9** and ca. +8.5 ppm for **5** and **7** (Table 1); in comparison, $\Delta\delta_{av}(C)$ values for the analogous IndNi complexes are ca. −2 ppm, indicating that the $\eta^5 \rightarrow \eta^3$ distortions in the Ind hapticity are much greater in the Pd complexes.

The chemical shifts of the symmetry-related carbons C1 and C3 (labeling shown in Chart 1 and on ORTEP diagrams) and their respective protons H1 and H3 also help shed light on the character of the Pd−Ind interaction. Inspection of the data in Table 1 shows that H3 resonates upfield of H1 by more than 1 ppm, while C3 resonates upfield of C1 by more than 20 ppm in all compounds. This phenomenon, which has also been observed for the analogous Ni complexes,[4] can be attributed to the relatively large difference in the trans influences of PR_3 and Cl ligands;[23] the nonsymmetrical Pd−C interactions resulting from this difference distort the Ind−Pd bonding toward a localized mode (η^1:η^2; Chart 1), which is manifested in different hybridizations at C1 (closer to sp^2) and C3 (closer to sp^3).

Another consequence of nonsymmetrical Pd−Ind interactions in solution is a high energy barrier for the rotation of the Ind ligand about the Pd−Ind axis. This was measured experimentally by studying the variable-temperature ^1H NMR spectra for complexes **4**, **7**, and **9**. The coalescence temperature (T_c) and the frequency differences ($\delta\nu$) measured for each pair of exchanging resonances (H1/H3, H4/H7, H5/H6) allowed us to estimate an average energy barrier for the rotation of indenyl rings using the Holmes−Gutowski equation.[24] The $\Delta G^{\ddagger}$ value of ca. 16.5 kcal/mol obtained for the complexes **4**, **7**, and **9** is similar to the values of ca. 16 kcal/mol measured for the analogous Ni−Cl complexes, whereas energy barriers of ca. 10 kcal/mol have been measured for the corresponding Ni−Me complexes.

The NMR data obtained for complex **10** were very similar to those found for other transition-metal η^1-indenyl complexes that have been reported in the literature.[12a,25] In the ^1H NMR spectrum of **10**, the proton on the carbon bonded directly to palladium appeared as a broad signal at 5.85 ppm, whereas the six remaining, nonequivalent Ind protons gave rise to three doublets at 6.77 ppm (H2), 7.32 ppm (H7), 7.89 ppm (H4) and one multiplet between 7.02 and 7.12 ppm for H3, H5, and H6. In the ^{13}C NMR spectrum, the chemical shift of the signal for C1 (44.1 ppm) differs substantially from that of the η-Ind complexes **4**, **5**, and **7**−**9**.

Solid-State Structural Studies. X-ray crystallographic analyses of the IndPd complexes prepared during the course of this work were undertaken to study the type of Ind−Pd interaction present in each compound (e.g., η^3 versus η^1 in **6** and **10**) and the influence on Ind hapticity of the auxiliary ligands (e.g., μ-Cl in **6** versus PR_3 and Cl in **4**, **5**, **7**, and **9**), phosphine substituents (**4** versus **7** and **9**),[26] and Ind substituent (**4** versus **5**). The ORTEP views for these complexes are shown in Figures 1−3, while crystal data and details of the diffraction experiments are listed in Table 2 (for **4**, **5**, **7** and **9**) and Table 3 (for **6** and **10**). A selection of bond distances and angles is given in Table 4 (for **4**, **5**, **7**, and **9**)[27] and Table 5 (for **6**[28] and **10**); the corresponding data for the compounds IndNi(PPh_3)Cl (**11**)[5a] and (1-Me-Ind)Ni(PPh_3)Cl (**12**)[5c] are also included in Table

(21) Merda, J. S.; Kacmarcik, R. T.; Engen, D. V. *J. Am. Chem. Soc.* **1986**, *108*, 329.

(22) Kohler, F. H. *Chem. Ber.* **1974**, *107*, 570.

(23) The difference in the chemical shifts of the H1/H3 signals is much larger in **4** (ca. 2 ppm) than in **7**−**9** (ca. 1 ppm). This is partially caused by the anisotropic current effects of the PPh_3 phenyl rings. This same phenomenon is clearly evident in the Ni complex **11**, for which the chemical shift difference between H1 and H3 signals is greater than 2.5 ppm (Table 1). We believe that the reason for the smaller anisotropic shift in the Pd complexes is the longer Pd−PPh_3 and Pd−Ind bond distances, which place H3 farther from the Ph rings of PPh_3 (by ca. 0.2 Å).

(24) Abraham. R. J.; Loftus, P. *Proton and Carbon-13 NMR Spectroscopy*; Wiley: New York, 1985; Chapter 7, pp 165−168, eq 7.11: ($RT_c = 22.96 + \ln(T_c/\delta\nu)$).

(25) (a) Casey, C. P.; O'Connor, J. M. *Organometallics* **1985**, *4*, 384. (b) Hermmann, W. A.; Kuhn, F. E.; Romao, C. C. *J. Organomet. Chem.* **1995**, *489*, C56. (c) O'Hare, D. *Organometallics* **1987**, *6*, 1766.

(26) We have also studied the solid-state structure of the PMe_3 analogue, complex **8**, but the low quality of the crystal results have precluded their inclusion here.

(27) The unit cells of complexes **4**, **7**, and **9** contain two independent molecules differing from each other by the orientation of the phosphine ligand in each case. In the case of **7** and **9**, the distances and angles are quite similar and have been averaged; in the case of complex **4**, however, the distances and angles of the two molecules are too dissimilar to allow averaging.

(28) The unit cell of complex **6** contains four independent half-molecules; the distances and angles are similar and have been averaged.

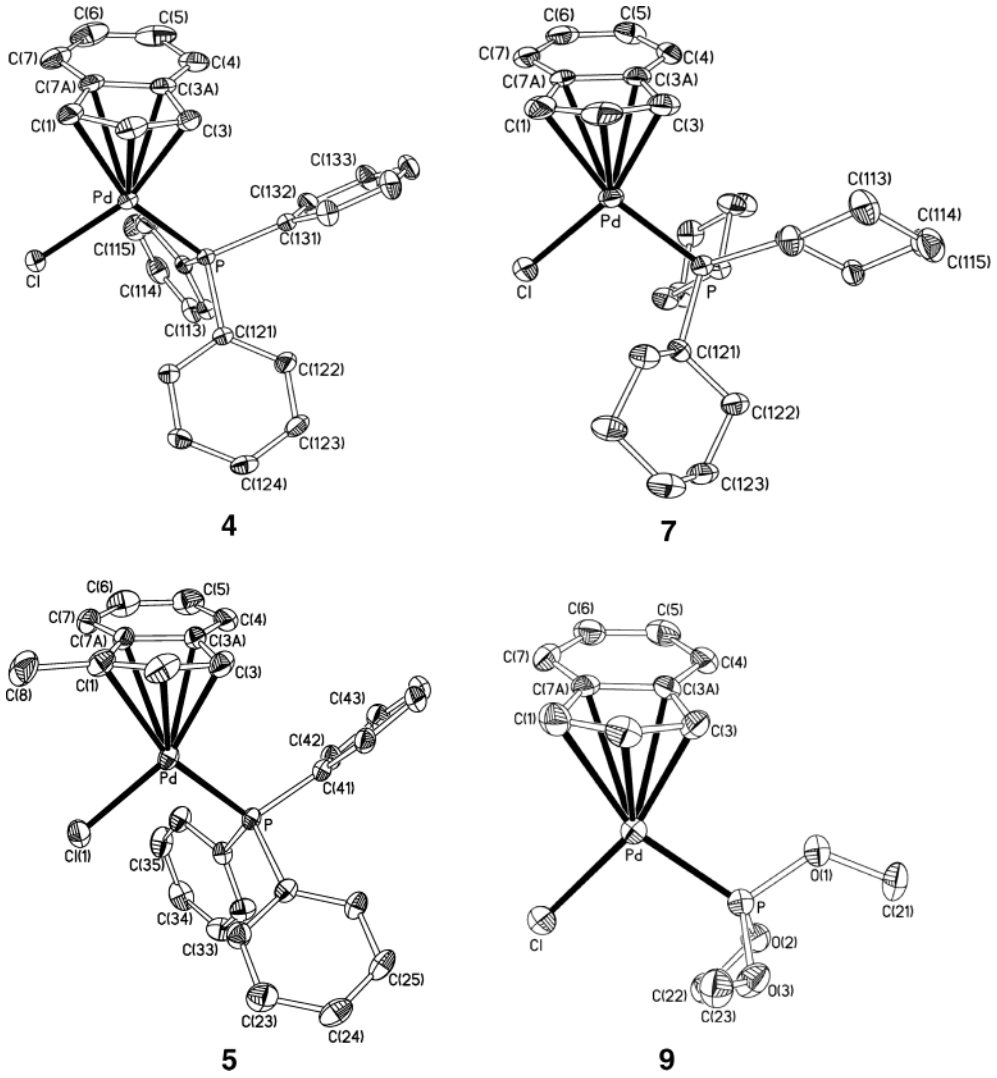

Figure 1. ORTEP views of complexes **4**, **5**, **7**, and **9**. Thermal ellipsoids are shown at 30% probability, and hydrogen atoms are omitted for clarity.

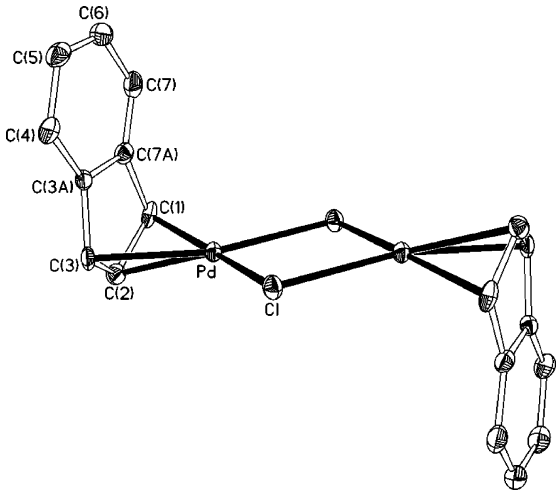

Figure 2. ORTEP view of complex **6**. Thermal ellipsoids are shown at 30% probability, and hydrogen atoms are omitted for clarity.

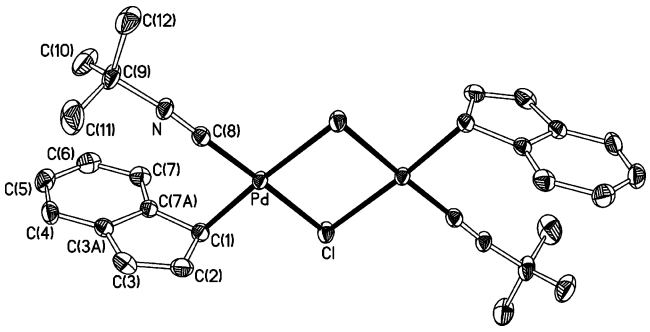

Figure 3. ORTEP view of complex **10**. Thermal ellipsoids are shown at 30% probability, and hydrogen atoms are omitted for clarity.

4 to facilitate structural comparisons between the Pd and Ni complexes.

The overall geometry around Pd in **10** is very nearly square planar (less than 5° deviation in all angles) but much more irregular in the remaining compounds. The largest structural distortion in the latter compounds arises from the small C(1)−Pd−C(3) angle of ca. 61°, which is fairly similar to the corresponding value of ca. 66° in the analogous Ni complexes. It is instructive to begin the structural discussion of Ind hapticity with the structures of the η-Ind complexes; the main structural features of complex **10** will be discussed last.

The metal center in all of the η-Ind complexes is within reasonable bonding distance from the P, Cl, C(1), C(2), and C(3) atoms but considerably farther away from

Table 2. Crystal Data and Data Collection and Structure Refinement Parameters of 4, 5, 7, and 9

	4	**5**	**7**	**9**
formula	$C_{27}H_{22}ClPPd$	$C_{28}H_{24}ClPPd.CH_2Cl_2$	$C_{27}H_{40}ClPPd$	$C_{12}H_{16}O_3ClPPd$
mol wt	519.27	618.218	537.41	381.07
cryst color, habit	red, block	red, block	orange, plate	red, block
cryst dimens, mm	0.08 × 0.25 × 0.33	0.30 × 0.34 × 0.47	0.02 × 0.11 × 0.65	0.11 × 0.12 × 0.18
symmetry	triclinic	monoclinic	monoclinic	monoclinic
space group	$P\bar{1}$	$P2_1/c$	$P2_1$	$P2_1/c$
a, Å	9.99970(10)	14.3388(1)	11.6214(3)	14.8857(4)
b, Å	14.5450(2)	11.0454(1)	19.4114(5)	17.2545(4)
c, Å	17.2588(2)	17.7748(1)	11.8247(3)	11.1260(4)
α, deg	65.630(1)	90	90	90
β, deg	83.151(1)	108.156(1)	102.441(2)	91.905(2)
γ, deg	89.093(1)	90	90	90
Z	4	4	4	8
D(calcd), g cm^{-3}	1.520	1.535	1.370	1.661
diffractometer	Bruker AXS SMART 2K			
temp, K	223(2)			
λ(Cu Kα), Å	1.541 78			
μ, mm^{-1}	8.421	9.035	7.336	13.255
scan type	*ω* scan			
F(000)	1048	1248	1120	1520
θ_{max} (deg)	72.90	72.90	72.93	73.03
h,*k*,*l* ranges	$-12 \le h \le 12$ $-17 \le k \le 17$ $-21 \le l \le 21$	$-17 \le h \le 17$ $-13 \le k \le 13$ $-22 \le l \le 21$	$-23 \le h \le 23$ $-14 \le k \le 14$ $-23 \le l \le 23$	$-18 \le h \le 18$ $-21 \le k \le 21$ $-10 \le l \le 12$
no. of rflns used ($I > 2\sigma(I)$)	7969	4825	8753	4016
abs cor	multiscan SADABS			
T(min, max)	0.1200, 0.5100	0.0630, 0.0670	0.4370, 0.8640	0.1850, 0.2330
$R(F^2 > 2\sigma(F^2))$, $R_w(F^2)$	0.0322, 0.0885	0.0521, 0.1385	0.0426, 0.0994	0.0883, 0.2194
GOF	1.027	1.029	1.012	1.030
Flack param			0.022(7)	

Table 3. Crystal Data and Data Collection and Structure Refinement Parameters of 6 and 10

	6	**10**
formula	$C_{18}H_{14}Cl_2Pd_2$	$C_{14}H_{16}ClNPd$
mol wt	513.99	340.13
cryst color, habit	orange, needle	orange, block
cryst dimens, mm	0.15 × 0.25 × 0.50	0.08 × 0.10 × 0.39
symmetry	triclinic	monoclinic
space group	$P\bar{1}$	$P2_1/c$
a, Å	10.2103(6)	6.37760(10)
b, Å	12.5513(7)	13.9174(3)
c, Å	12.7249(7)	16.0809(3)
α, deg	87.970(1)	90
β, deg	78.209(1)	90.26(10)
γ, deg	89.497(1)	90
V, Å^3	1592.32(16)	1427.32(5)
Z	4	4
D(calcd), g cm^{-3}	2.141	1.583
diffractometer	Bruker AXS SMART 1K	Bruker AXS SMART 2K
temp, K	173(2)	223(2)
λ, Å	0.7107	1.541 78
μ, mm^{-1}	2.580	12.018
scan type	*ω* scan	*ω* scan
F(000)	992	680
θ_{max} deg	29.62	72.88
h,*k*,*l* range	$-14 \le h \le 14$ $-17 \le k \le 17$ $-17 \le l \le 17$	$-7 \le h \le 6$ $-17 \le k \le 16$ $-19 \le l \le 19$
no. of rflns used ($I > 2\sigma(I)$)	11 089	2498
abs cor	multiscan SADABS	
T(min, max)	0.53, 0.86	0.27, 0.38
$R(F^2 > 2\sigma(F^2))$, $R_w(F^2)$	0.0596, 0.1451	0.0263, 0.0680
GOF	0.894	1.018
BASF, %	17.6	

C3a and C7a. The extent of M−Ind interaction can be most conveniently estimated by the relative values of the "slip" parameter Δ(M−C), which corresponds to the difference between the average M−C distances from the two allylic carbons (C1, C3) and the two quaternary carbons (C3a, C7a); the hinge and fold angles (HA, FA, as defined in Table 4) are also useful for this purpose.[29] Interestingly, the Δ(M−C), HA, and FA values observed for complex **6** (Table 5) are larger than those of all known monomeric Pd complexes (Table 4), implying a larger degree of $\eta^5 \rightarrow \eta^3$ distortion in this complex. Since **6** is the only neutral Pd^{II}Ind compound not bearing a phosphine ligand, it is tempting to speculate on the importance of Pd→phosphine *π*-back-bonding in these complexes; however, the closeness of the structural parameters for complexes **4**, **7**, and **9**, bearing phosphines of different *π* acidities, seems to discount this possibility.

Let us turn now to comparing the structural features of the monomeric Ni and Pd complexes. The data listed in Table 4 show that the Pd complexes exhibit significantly larger values of Δ(M−C) (ca.. 0.32−0.39 Å versus 0.25 Å) and HA/FA (ca. 13.3−15.5° versus 10.9−11.8°), implying that $\eta^5 \rightarrow \eta^3$ slip-fold distortions are more pronounced in IndPd complexes relative to their analogous Ni counterparts. The same trend is observed in the reported structural data for previously studied IndPd complexes.[4] For example, the Δ(M−C) values for IndPd(PMe$_3$)(CH$_2$SiMe$_3$)[12b] and its close analogue (1-Me-Ind)Ni(PMe$_3$)(CH$_3$)[8b] are 0.39 and 0.27 Å, respectively. The generally weaker Pd−Ind interaction presumably reflects the more electron rich nature of Pd versus Ni; this assertion is borne out by the results of our electrochemical studies (vide infra).

As expected on the basis of the unequal trans influences of PR$_3$ and Cl ligands, the Pd−Ind interactions in **4**, **5**, **7**, and **9** are also quite nonsymmetrical: Pd−C(3) < Pd−C(1) by about 15−40 times the esd values. The net result of this distortion is a partial localization of bonding in the allyl moiety of the Ind ligand (i.e., η^1:

(29) The Δ(M−C), HA, and FA values for a range of Ind complexes are given in refs 19 and 20. The corresponding data for group 10 complexes are given in ref 4.

Table 4. Selected Bond Distances (Å) and Angles (deg) for 4, 5, 7, and 9 and the Analogous Nickel Complexes 11 and 12

	4[27]		**11**	**7**[27]	**9**[27]	**5**	**12**
M−P	2.2785(6)	2.2673(6)	2.1835(7)	2.2702(14)	2.216(3)	2.2649(8)	2.1782(11)
M−Cl	2.3474(6)	2.3560(7)	2.1822(7)	2.3521(13)	2.355(2)	2.3585(8)	2.1865(10)
M−C1	2.244(2)	2.282(3)	2.094(2)	2.290(7)	2.339(10)	2.314(4)	2.137(2)
M−C2	2.186(2)	2.209(3)	2.061(2)	2.193(6)	2.198(10)	2.228(4)	2.072(2)
M−C3	2.192(2)	2.165(3)	2.042(2)	2.179(6)	2.120(9)	2.144(4)	2.026(3)
M−C3a	2.607(2)	2.544(3)	2.318(2)	2.595(5)	2.570(10)	2.520(3)	2.308(2)
M−C7a	2.610(2)	2.580(2)	2.344(2)	2.647(6)	2.671(10)	2.586(3)	2.351(2)
C1−C2	1.404(4)	1.393(4)	1.399(4)	1.401(12)	1.397(16)	1.392(6)	1.403(4)
C2−C3	1.410(4)	1.413(4)	1.417(4)	1.430(10)	1.436(15)	1.419(6)	1.421(4)
C3−C3a	1.474(4)	1.468(4)	1.449(3)	1.454(9)	1.440(15)	1.479(6)	1.451(4)
C3a−C7a	1.415(4)	1.422(4)	1.422(3)	1.422(8)	1.413(14)	1.417(4)	1.417(4)
C7a−C1	1.464(4)	1.465(4)	1.459(3)	1.434(10)	1.463(15)	1.475(5)	1.457(4)
P−M−Cl	96.23(2)	97.04(2)	98.82(4)	95.89(6)	99.7(9)	97.56(3)	97.43(2)
C3−M−Cl	158.71(7)	160.78(8)	161.51(8)	161.1(2)	163.6(3)	159.4(1)	161.52(7)
C3-M−P	104.91(7)	101.75(8)	99.33(8)	102.5(2)	96.4(3)	102.9(1)	100.69(7)
C1−M−Cl	97.29(7)	99.48(8)	95.48(8)	100.5(2)	103.1(3)	98.1(1)	95.83(8)
C1−M−P	164.25(7)	161.72(8)	165.6(7)	163.4(2)	156.9(3)	132.1(1)	166.34(8)
C1-M−C3	61.4(1)	61.3(1)	66.5(1)	61.3(3)	61.1(4)	61.3(1)	66.3(1)
ΔM−C[a](Å)	0.39	0.39	0.26	0.39	0.39	0.32	0.25
HA[b] (deg)	15.49	14.58	10.9	15.49	15.54	14.72	11.00
FA[c] (deg)	14.84	14.40	11.7	14.03	15.57	13.32	11.80

[a] $\Delta(M-C) = 0.5\{(M-C3a + M-C7a)\} - 0.5\{(M-C1 + M-C3)\}$. [b] HA is the angle formed between the planes formed by the atoms C1, C2, C3 and C1, C3, C3a, C7a. [c] FA is the angle formed between the planes formed by the atoms C1, C2, C3 and C3a, C4, C5, C6, C7 and C7a.

Table 5. Selected Bond Distances (Å) and Angles (deg) for 6 and 10

6[28]		**10**	
Pd−C1	2.204(6)	Pd−C1	2.063(3)
Pd−C2	2.137(7)	Pd−C8	1.929(3)
Pd−C3	2.165(7)	Pd−Cl	2.3634(7)
Pd−C3a	2.640(7)	Pd−Cl#1	2.4580(7)
Pd−C7a	2.656(6)	C8−N	1.138(4)
C1−C2	1.424(10)	C9−N	1.463(3)
C2−C3	1.404(10)	C1−C2	1.477(5)
C3−C3a	1.491(9)	C1−C7a	1.495(4)
C3a−C7a	1.419(9)	C2−C3	1.349(5)
C7a−C1	1.479(9)	C3−C3a	1.435(4)
C1−Pd−C3	62.4(3)	C3a−C7a	1.408(4)
C1−Pd−Cl	165.88(18)	C1−Pd−C8	87.66(12)
Cl−Pd−Cl#1	87.06(6)	C8−Pd−Cl	177.77(8)
Cl#1-Pd−C3	165.34(18)	C1−Pd−Cl	90.37(9)
Pd−Cl−Pd#1	92.94(6)	C8−Pd−Cl#1	95.22(8)
Δ(M−C)	0.463	C1−Pd−Cl#1	176.25(8)
HA	17.30	Cl−Pd−Cl#1	86.79(2)
FA	16.39	Pd−Cl−Pd#1	93.21(2)
		C8−N−C9	171.3(3)
		N−C8−Pd	179.3(3)

η^2 distortion; Chart 1), which is also reflected in the nominally shorter C(1)−C(2) versus C(2)−C(3) distances. Moreover, the localization of bonding inside the Ind moiety is also reflected in the ^{1}H and ^{13}C{^{1}H} NMR chemical shifts of these complexes (vide supra); therefore, the solid-state hapticity of the Ind ligand in these Pd complexes is maintained in solution, as observed for the previously studied Ni complexes. Consistent with this correspondence between the solid-state and solution structures, we have noted a correlation between Δ(M−C) and $\Delta\delta(^{13}C)$ parameters of Ni and Pd complexes (Figure 4); a similar correlation has also been demonstated previously for a wide range of Ind complexes.[19]

In contrast to the η-Ind complexes discussed above, the Ind ligand in complex **10** adopts a η^1 coordination mode. This compound crystallizes in the centrosymmetric space group $P2_1/c$ and lies on an inversion center. The Pd center is surrounded by η^1-Ind, *t*-BuNC, and two μ-Cl ligands. As expected, the Pd−C8 distance (ca. 1.93 Å) is shorter than the Pd−C1 distance (ca. 2.06 Å). The Pd−Cl bond distances trans to η^1-Ind are longer (by ca. 10 esd values) than those trans to *t*-BuNC, indicating that η^1-Ind exerts a larger trans influence than *t*-BuNC. The remaining structural parameters for this complex are similar to those found in structurally characterized η^1-Ind complexes.[30] For example, the metal-bound carbon atom is sp^3 hybridized, as reflected in the C1−C7a (ca. 1.50 Å) and C1−C2 (ca. 1.48 Å) distances that are in the normal range for single C−C bonds, whereas the C2−C3 distance (ca. 1.35 Å) is in the expected range for a $C(sp^2)-C(sp^2)$ double bond.

The structural parameters for the isocyanide ligand (C8−N ≈ 1.14 Å, C8−N−C9 ≈ 171°) and the ν(CN) absorption band in **10** (2204 cm^{-1}), which is at higher energy than for the free ligand (2136 cm^{-1}), are consistent with little π-back-bonding. Similar ν(CN) values, Pd−C and C−N distances, and C−N−C angles have been reported for other Pd(II)−isocyanide complexes.[31] The IR data in particular indicate an increased C−N bond order, probably caused by a strong σ donation from the isocyanide ligand's lone pair to Pd with little or no π-back-donation.

Electrochemical Studies. Table 1 lists the reduction potentials obtained from the cyclic voltammetry (CV) studies carried out on complexes **4**, **5**, **7**, **8**, **11**, and **12**. The CV measurements of these complexes showed that they undergo two successive and irreversible one-electron reductions (presumably $M^{II} \rightarrow M^{I}$ and $M^{I} \rightarrow M^{0}$) at potentials ranging from −0.64 to −1.24 V for the first wave and from −1.05 to −1.64 V for the second. (In the case of complexes **8** and **12**, second reductions were too

(30) (a) Guérin, F.; Beddie, C. L.; Stephan, D. W.; Spence, E. v. H.; Wurz, R. *Organometallics* **2001**, *20*, 3466. (b) Deck, P. A.; Fronczek, F. R. *Organometallics* **2000**, *19*, 327. (c) Blenkiron, P.; Enright, G. D.; Taylor, N. J.; Carty, A. J. *Organometallics* **1996**, *15*, 2855. (d) Thorn, M. G.; Fanwick, P. E.; Chesnut, R. W.; Rothwell, I. P. *Chem. Commun.* **1999**, 2543. (e) Radius, U.; Sundermeyer, J.; Peters, K.; von Schering, H. G. Z. *Anorg. Allg. Chem.* **2002**, *628*, 1226.

(31) (a) Otsuka, S.; Nakamura, A.; Yoshida, T. *J. Am. Chem. Soc.* **1969**, *91*, 7196. (b) Crociani, B.; Boschi, T.; Belluco, U. *Inorg. Chem.* **1970**, *9*, 2021. (c) Cherwinski, W. J.; Clark, H. C.; Manzer, L. E. *Inorg. Chem.* **1972**, *11*, 1511. (d) De Munno, G.; Bruno, G.; Grazia Arena, C.; Drommi, D.; Faraone, F. *J. Organomet. Chem.* **1993**, *450*, 263.

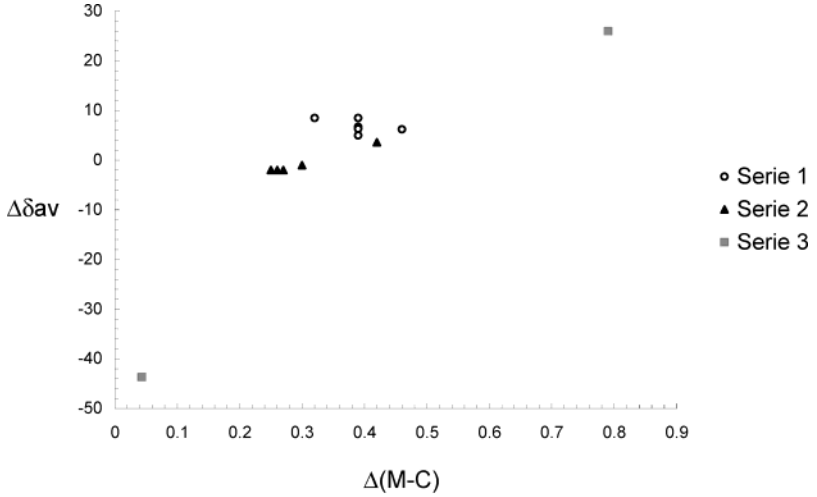

	Complex	(Δ(M-C), Δδ)
Serie 1 ○	(Ind)Pd(PPh_3)Cl	(0.39, 6.7)
	(1-Me-Ind)Pd(PPh_3)Cl	(0.32, 8.5)
	(Ind)Pd(PCy_3)Cl	(0.39, 8.5)
	(Ind)Pd($P(OMe)_3$)Cl	(0.39, 6.3)
	(Ind)Pd(PMe_3)(CH_2-$SiMe_3$) [12b]	(0.39, 5.0)
	{(Ind)Pd(μ-Cl)}$_2$	(0.46, 6.2)
Serie 2 ▲	$Ni(Ind)_2$ [22]	(0.42, 3.6)
	(Ind)Ni(PPh_3)Cl [5a]	(0.25, -2)
	(1-Me-Ind)Ni(PPh_3)Cl [5c]	(0.26, -2)
	(1-Me-Ind)Ni(PCy_3)Cl [5c]	(0.30, -1)
	(1-Me-Ind)Ni(PMe_3)Cl [5c]	(0.27, -2)
Serie 3 ■	(η^5-Ind)$_2$Fe [20]	(0.04, -43)
	(η^3-Ind)Ir(PMe_3)$_3$ [21]	(0.79, 26)

Figure 4. Correlation between $\Delta\delta_{av}$ (ppm) and Δ(M−C) (Å).

weak to be observed.) The relative reduction potentials of these complexes indicate that the Ind−Ni complexes are more easily reduced than the Ind−Pd compounds; this is consistent with the solid-state data, which implied more electron rich Pd centers. Inspection of the electrochemical data also shows that the E_{red} values for the species **8** ($E_{red1} = -1.24$ V) and **4** ($E_{red1} = -0.94$ V, $E_{red2} = -1.41$ V) follow the donor ability of the phosphine (PMe_3 > PPh_3); the reduction potential of the PCy_3 analogue **7** is less negative ($E_{red1} = -1.07$ V, $E_{red2} = -1.64$ V) than that of the PMe_3 analogue, presumably due to a less effective electron donation caused by the greater steric volume of PCy_3.

Catalytic Reactivities of IndPd Complexes. Recent work in our group has shown that the complexes (Ind)Ni(PR_3)Cl are inert toward hydrosilanes and olefins, but they catalyze the dehydrogenative polymerization of $PhSiH_3$,[8a] hydrosilylation of olefins and ketones,[9] and polymerization of olefins[6] in the presence of excess MAO. We have briefly probed the reactivities of some of the IndPd species reported here as a preliminary comparison of their reactivities relative to those of their Ni analogues. Thus, the reactions of complexes **4**−**7** with excess $PhSiH_3$ led to an instantaneous darkening of the reaction mixture and the evolution of a gas, indicating that the Pd complexes react with this substrate in the absence of cocatalysts. Careful NMR monitoring of mixtures of the complexes **4**−**6** and 200 equiv of $PhSiH_3$ in a C_6D_6 solution indicated the disappearance of the substrate Si−H and Ph-Si signals (ca. 20% over 20 min); curiously, however, no new ^{1}H signal was detected for the anticipated products of the reaction (i.e., $(PhSiH)_n$). Monitoring the $^{31}P\{^1H\}$ NMR spectra during the course of the reaction showed only a broad signal at ca. −1.2 ppm (assigned to exchanging PPh_3); the spectrum at the end of the reaction signaled the presence of free PPh_3 (ca. −5 ppm) and O=PPh_3 (ca. +25 ppm).

Additional information was obtained from monitoring the reaction of the Pd complexes with stoicheometric quantities of $PhSiH_3$. Thus, the ^{1}H NMR spectrum of the reaction of **4** with $PhSiH_3$ (ca. 1:1) showed free IndH, $(PhSiH_2)_2$ (singlet at ca. 4.46 ppm assigned to Si−*H* of the dimer),[8b] and Ph_2SiH_2 (singlet at ca. 5.1 ppm) in addition to other, unassigned peaks; the $^{31}P\{^1H\}$ NMR spectrum of the final mixture showed only $Pd(PPh_3)_n$ (ca. +24 ppm). On the other hand, the analogous reaction with **6** led to the complete consumption of $PhSiH_3$ and formation of indene and indane (hydrogenated indene), in addition to a number of minor signals; significantly, no trace of the anticipated Si-containing products (e.g., dimer, oligomer, and Ph_2SiH_2) was observed.

Evidently, these reactions follow a complicated and as yet not well-understood course. The available data allow us, however, to offer the following speculation: (a)

initial reaction of $PhSiH_3$ with the Pd precursors results in the elimination of IndH and the formation of Pd^0; (b) in the presence of PPh_3 ligands (reaction with **4**), the resulting $Pd(PPh_3)_n$ can react with $PhSiH_3$ to promote both dehydrogenative Si−Si bond formation and redistribution, whereas these reactions do not seem to occur in the absence of phosphine (reaction with **6**). It is noteworthy that, unlike the case of the Ni complexes, the presence of MAO did not change the course of the reactions involving IndPd complexes. Finally, no hydrosilylation of styrene was observed in the presence of $PhSiH_3$ and the complexes **4**−**6**, with or without MAO.

We have also studied the catalytic activities of our Pd complexes in the polymerization of ethylene. Thus, we found that complexes **4** and **6** produced polyethylene (PE) with modest activities (204 and 124 kg of PE/((mol of Pd) h), respectively; polymerization conditions 600 equiv of MAO, ethylene-saturated toluene with $P_{ethylene} \approx 16$ atm, 60 °C, 30 min). It appears, therefore, that these Pd complexes are more active in this reaction relative to their Ni counterparts; for instance, the complex (1-Me-Ind)Ni(PPh_3)Cl showed an activity of about 50 kg of PE/((mol of Ni) h) under similar conditions (except for $P_{ethylene} \approx 5$ atm).

Conclusion

Two routes have been developed for the preparation of indenylpalladium complexes. The first route, involving the reaction of $(PhCN)_2PdCl_2$ with LiInd and PPh_3, gives modest yields, while the second route, the addition of PR_3 to the dimeric compound $\{(\eta^3\text{-Ind})Pd(\mu\text{-Cl})\}_2$ (**6**), gives good yields of $(\eta\text{-Ind})Pd(PR_3)Cl$. The dimeric derivate $\{(\eta^1\text{-Ind})(t\text{-BuNC})Pd(\mu\text{-Cl})\}_2$ (**10**), which is the first example of an isolated $(\eta^1\text{-Ind})Pd$ complex, was obtained from the reaction of *t*-BuNC with **6**. The structural studies have revealed significant differences in the hapticity of the Ind ligand (both in solution and in the solid state) between the Pd and Ni complexes, with the IndPd complexes displaying greater $\eta^5 \rightarrow \eta^3$ slippage. Electrochemical measurements have confirmed that the Pd centers are more electron rich than their Ni analogues. Preliminary reactivity studies have shown that the Pd complexes are also somewhat more reactive, but systematic studies are needed to delineate the exact differences in the chemistry of these complexes. Studies are underway to probe and expand the scope of the reactions catalyzed by the IndPd compounds.

Experimental Section

General Comments. All manipulations and experiments were performed under an inert atmosphere using standard Schlenk techniques and/or a nitrogen-filled glovebox. Dry, oxygen-free solvents were prepared by distillation from appropriate drying agents and employed throughout. The syntheses of $(PhCN)_2PdCl_2$[32] and $(PMe_3)_2PdCl_2$[33] were carried out according to published procedures; all other reagents used in the experiments were obtained from commercial sources and used as received. The elemental analyses were performed by the Laboratoire d'Analyse Elémentaire (Université de Montréal). Bruker ARX400, AV400, AMX300, and AV300 spectrometers were employed for recording ^1H (400 and 300 MHz), $^{13}C\{^1H\}$ (100.56 and 75.42 MHz), and $^{31}P\{^1H\}$ NMR spectra (161.92 MHz) at ambient temperature. The NMR spectra are referenced to (a) the residual solvent resonances for the ^1H and $^{13}C\{^1H\}$ spectra, and (b) 85% H_3PO_4 (0 ppm) for the $^{31}P\{^1H\}$ spectra. The ethylene polymerization experiments have been realized as described in a recent paper.[6d]

Crystal Structure Determinations. The crystal data for complexes **4**−**7**, **9**, and **10** were collected on Bruker AXS Smart 2K and 1K (for **6**) diffractometers using SMART.[34] Graphite-monochromated Cu Kα radiation was used at 223(2) K for all crystals except that of **6**, for which the radiation used was Mo Kα at 173(2) K. Cell refinement and data reduction were done using SAINT.[35] All structures were solved by direct methods using SHELXS97[36] and difmap synthesis using SHELXL97;[37] the refinements were done on F^2 by full-matrix least squares. All non-hydrogen atoms were refined anisotropically, while the hydrogens (isotropic) were constrained to the parent atom using a riding model. The crystal structure of **6** presented two twin components which have been described by a matrix obtained with the Gemini program.[38] In the case of complex **9**, the Cu radiation employed resulted in relatively high absorption and gave less satisfactory data; using SADABS[39] improved the results, but the *R* factor for this structure remained fairly high (ca. 8.8%). The crystal data and experimental details are listed in Tables 2 and 3, while selected bond distances and angles are listed in Tables 4 and 5.

Synthesis of $\{(\eta^3\text{-Ind})Pd(\mu\text{-Cl})\}_2$ (6). The original synthesis of this compound was reported previously;[10] we have used the following procedure, which has been reported by Lin and Boudjouk.[18] Into a Schlenk flask, under nitrogen, Na_2PdCl_4 (6.5 g, 21.9 mmol) and 200 mL of ethanol were heated to reflux until a clear brown solution was obtained. After the solution was cooled to room temperature, 1-$SiMe_3$-Ind (4.7 g, 25 mmol) was added to produce a brown solid, which precipitated gradually. After it was stirred for 20 min, the mixture was filtered and the collected solid washed successively with distilled water, Et_2O, and ethanol to give the compound $\{(\eta^3\text{-Ind})Pd(\mu\text{-Cl})\}_2$ (**6**; 4.9 g, 87%) as a brown powder. Recrystallization of a small portion of this solid from a cold CH_2Cl_2/Et_2O solution yielded crystals suitable for X-ray diffraction studies. ^1H NMR ($CDCl_3$, 300 MHz): δ 6.88−6.83 (m, H_{4-7}), 5.84 (br, H_{1-3}). $^{13}C\{^1H\}$ NMR (Me_2SO-d_6, 75.40 MHz): δ 136.9 (s, C_{3a-7a}), 127.4 (s, C_{4-7}), 118.8 (s, $C_{5,6}$), 114.0 (s, C_2), 85.4 (s, C_{1-3}).

Synthesis of (Ind)Pd(PPh_3)Cl (4). Method A. An Et_2O solution (60 mL) of IndLi (320 mg, 2.61 mmol) was added dropwise to a stirred suspension of $(PhCN)_2PdCl_2$ (1 g, 2.61 mmol) in Et_2O (80 mL) at − 78 °C. The mixture was warmed to room temperature and stirred for 30 min. After PPh_3 was added (410 mg, 1.56 mmol), the resultant dark red mixture was stirred for approximately 30 min, filtered through a small pad of Celite, and concentrated. A red-brown powder precipitated and was isolated by filtration (501 mg, 60%).

Method B. PPh_3 (1.14 g, 4.3 mmol) was added to a stirred Et_2O suspension (110 mL) of $\{(\eta^3\text{-Ind})Pd(\mu\text{-Cl})\}_2$ (**6**; 1.24 g, 2.4 mmol) at room temperature. After it was stirred for 1 h, the resulting red solution was concentrated to ca. 60 mL. A red-brown powder precipitated and was isolated by filtration (2.02 g, 89%). Recrystallization of a small portion of this solid from

(32) Anderson, G. K.; Lin, M. *Inorg. Synth.* **1990**, *28*, 60.
(33) Klein, H.-F.; Zettel, B.; Flörke, U.; Haupt, H.-J. *Chem. Ber.* **1992**, *125*, 9.
(34) SMART, Release 5.059; Bruker Molecular Analysis Research Tool, Bruker AXS Inc., Madison, WI 53719-1173, 1999.
(35) SAINT, Release 6.06; Integration Software for Single-Crystal Data; Bruker AXS Inc., Madison, WI 53719-1173, 1999.
(36) Sheldrick, G. M. SHELXS: Program for the Solution of Crystal Structures; University of Göttingen, Göttingen, Germany, 1997.
(37) Sheldrick, G. M. SHELXL: Program for the Refinement of Crystal Structures; University of Göttingen, Göttingen, Germany, 1997.
(38) GEMINI, version 1.02, Twinning Solution Program; Bruker AXS Inc., Madison, WI 53711-5373, 1999.
(39) Sheldrick, G. M. SADABS, Bruker Area Detector Absorption Corrections; Bruker AXS Inc., Madison, WI 53719-1173, 1997.

a cold CH_3CN/hexane solution yielded crystals suitable for X-ray diffraction studies and elemental analysis. ^{1}H NMR ($CDCl_3$, 300 MHz): δ 7.56−7.39 (m, PPh_3), 7.26 (d, $^3J_{H-H}$ = 7.5 Hz, H_7), 7.07 (t, $^3J_{H-H}$ = 7.5 Hz, H_6), 6.87 (t, $^3J_{H-H}$ = 7.4 Hz, H_5), 6.73 (t, $^3J_{H-H}$ = 6.4 Hz, H_2), 6.51 (d, $^3J_{H-H}$ = 9.9 Hz, H_1), 6.38 (d, $^3J_{H-H}$ = 7.2 Hz, H_4), 4.57 (t, $^3J_{H-H}$ = 2.01 Hz, H_3). $^{13}C\{^1H\}$ NMR ($CDCl_3$, 100.56 MHz): δ 136.16 (s, C_{7a}), 135.18 (s, C_{3a}), 134.30 (d, $^2J_{C-P}$ = 12.4 Hz, C_{ortho}), 132.00 (d, $^1J_{C-P}$ = 45.57 Hz, C_{ipso}), 130.95 (s, C_{para}), 128.96 (d, $^3J_{C-P}$ = 10.6 Hz, C_{meta}), 127.45 (s, C_6), 126.55 (s, C_5), 119.77 (s, C_7), 116.91 (s, C_4), 111.56 (d, $^2J_{C-P}$ = 22.7 Hz, C_2), 97.23 (d, $^2J_{C-P}$ = 22.7 Hz, C_1), 79.88 (s, C_3). $^{31}P\{^1H\}$ NMR ($CDCl_3$, 121.49 MHz): δ 28.58 (s). $^{31}P\{^1H\}$ NMR (C_6D_6, 121.49 MHz): δ 27.98 (s). Anal. Calcd for $C_{27}H_{22}ClPPd$: C, 62.45; H, 4.27. Found: C, 61.91; H, 4.56.

Synthesis of (1-Me-Ind)Pd(PPh_3)Cl (5). An Et_2O solution (60 mL) of 1-Me-IndLi (355 mg, 2.61 mmol) was added dropwise to a stirred suspension of $(PhCN)_2PdCl_2$ (1 g, 2.61 mmol) in Et_2O (80 mL) at −78 °C. The mixture was warmed to room temperature and then stirred for 30 min. After PPh_3 was added (410 mg, 1.56 mmol), the resultant dark red mixture was stirred approximately 30 min, filtered through a small pad of Celite, and concentrated. A red-brown precipitate was isolated by filtration (501 mg, 60%). Recrystallization of a small portion of this solid from a cold CH_2Cl_2/hexane solution yielded crystals suitable for X-ray diffraction studies and elemental analysis. ^{1}H NMR (C_6D_6, 400 MHz): δ 7.50−7.61 (m, PPh_3), 7.03 (d, $^3J_{H-H}$ = 7.7 Hz, H_7), 6.90−6.95 (m, PPh_3), 6.94 (t, $^3J_{H-H}$ = 7.6 Hz, H_6), 6.75 (t, $^3J_{H-H}$ = 7.4 Hz, H_5), 6.23 (d, $^3J_{H-H}$ = 7.5 Hz, H_4), 6.12 (d, $^3J_{H-H}$ = 2.7 Hz, H_2), 4.28 (d, $^3J_{H-H}$ = 2.7 Hz, H_3), 2.04 (d, $^3J_{H-P}$ = 10.4 Hz, Me). ^{1}H NMR ($CDCl_3$, 400 MHz): δ 7.39−7.45 (m, PPh_3), 7.19 (d, $^3J_{H-H}$ = 7.3 Hz, H_7), 7.08 (t, $^3J_{H-H}$ = 7.3 Hz, H_6), 6.86 (t, $^3J_{H-H}$ = 7.6 Hz, H_5), 6.49 (d, $^3J_{H-H}$ = 2.8 Hz, H_2), 6.24 (d, $^3J_{H-H}$ = 7.4 Hz, H_4), 4.46 (d, $^3J_{H-H}$ = 2.8 Hz, H_3), 2.05 (d, $^3J_{H-P}$ = 10.6 Hz, Me). $^{13}C\{^1H\}$ NMR (C_6D_6, 100.56 MHz): δ 138.96 (d, $^3J_{C-P}$ = 4.1 Hz, C_{7a}), 136.37 (d, $^3J_{C-P}$ = 0.69 Hz, C_{3a}), 135.02 (d, $^2J_{C-P}$ = 12.5 Hz, C_{ortho}), 133.85 (d, $^1J_{C-P}$ = 43.7 Hz, C_{ipso}), 131.01 (s, C_{para}), 129.13 (d, $^3J_{C-P}$ = 10.4 Hz, C_{meta}), 126.95 (s, C_6), 126.84 (s, C_5), 118.70 (s, C_7), 116.48 (s, C_4), 113.33 (d, $^2J_{C-P}$ = 21.5 Hz, C_1), 111.56 (d, $^2J_{C-P}$ = 5.5 Hz, C_2), 76.46 (s, C_3), 13.09 (d, $^3J_{C-P}$ = 5.6 Hz, *Me*). $^{31}P\{^1H\}$ NMR (C_6D_6, 161.92 MHz): δ 30.03 (s). $^{31}P\{^1H\}$ NMR ($CDCl_3$, 161.92 MHz): δ 29.67 (s). Anal. Calcd for $C_{28}H_{24}ClPPd\cdot{}^2/_3LiCl$: C, 59.89; H, 4.54. Found: C, 59.32; H, 4.46.

Synthesis of (Ind)Pd(PCy_3)Cl (7). A stirred Et_2O solution (30 mL) of PCy_3 (436 mg, 1.56 mmol) was added to a stirred Et_2O suspension (110 mL) of $\{(\eta^3\text{-Ind})Pd(\mu\text{-Cl})\}_2$ (**6**; 1.24 g, 2.4 mmol) at room temperature. After it was stirred for 45 min, the resulting red solution was filtered and then concentrated to 60 mL. An orange powder precipitated and was isolated by filtration (710 mg, 85%). Recrystallization of a small portion of this solid from a cold CH_3CN/hexane solution yielded crystals suitable for X-ray diffraction studies and elemental analysis. ^{1}H NMR (C_6D_6, 300 MHz): δ 7.13 (d, $^3J_{H-H}$ = 7.6 Hz, H_7), 6.92 (t, $^3J_{H-H}$ = 7.2 Hz, H_6), 6.88 (d, $^3J_{H-H}$ = 6.9 Hz, H_4), 6.81 (t, $^3J_{H-H}$ = 7.1 Hz, H_5), 6.33 (t, $^3J_{H-H}$ = 3.06 Hz, H_2), 6.21 (d, $^3J_{H-H}$ = 9.4 Hz, H_1), 5.11 (s, H_3), 1.98−1.08 (m, PCy_3). $^{13}C\{^1H\}$ NMR (C_6D_6, 75.40 MHz): δ 137.85 (s, C_{7a}), 137.15 (s, C_{3a}), 126.34 (s, C_6), 124.61 (s, C_5), 119.84 (s, C_7), 117.83 (s, C_4), 110.87 (d, $^2J_{C-P}$ = 5.2 Hz, C_2), 94.26 (d, $^2J_{C-P}$ = 21.8 Hz, C_1), 70.94 (d, $^2J_{C-P}$ = 3.4 Hz, C_3), 35.35 (d, $^1J_{C-P}$ = 19.8 Hz, C_{ipso}), 30.2 (d, $^2J_{C-P}$ = 11.1 Hz, C_{ortho}), 27.69 (d, $^3J_{C-P}$ = 11.7 Hz, C_{meta}), 27.61 (d, $^3J_{C-P}$ = 10.9 Hz, C_{meta}), 6.61 (s, C_{para}). $^{31}P\{^1H\}$ NMR (C_6D_6, 161.92 MHz): δ 49.04 (s). $^{31}P\{^1H\}$ NMR ($CDCl_3$, 161.92 MHz): δ 48.34 (s). Anal. Calcd for $C_{27}H_{40}ClPPd$: C, 60.34; H, 7.50. Found: C, 59.92; H, 7.66.

Synthesis of (Ind)Pd(PMe_3)Cl (8). PMe_3 (161 μL, 1.6 mmol) was syringed into a stirred Et_2O suspension (50 mL) of $\{(\eta^3\text{-Ind})Pd(\mu\text{-Cl})\}_2$ (**6**; 500 mg, 0.97 mmol) at room temperature. After it was stirred for 45 min, the resulting red solution was filtered and then concentrated to 60 mL. An orange powder precipitated and was isolated by filtration (380 mg, 73%). Recrystallization of a small portion of this solid from a cold toluene/hexane solution yielded crystals suitable for X-ray diffraction studies and elemental analysis. ^{1}H NMR ($CDCl_3$, 400 MHz): δ 7.20 (d, $^3J_{H-H}$ = 7.6 Hz, H_7), 7.04 (t, $^3J_{H-H}$ = 7.0 Hz, H_6), 6.98−6.93 (m, H_5 and H_4), 6.64 (t, $^3J_{H-H}$ = 2.9 Hz, H_2), 6.42 (d, $^3J_{H-H}$ = 9.5 Hz, H_1), 5.26 (s, H_3), 1.48 (d, $^2J_{H-P}$ = 11.4 Hz, PMe_3). $^{13}C\{^1H\}$ NMR (C_6D_6, 75.40 MHz): δ 136.34 (s, C_{7a}), 134.89 (s, C_{3a}), 126.67 (s, C_6), 125.84 (s, C_5), 119.55 (s, C_7), 116.23 (s, C_4), 111.16 (s, C_2), 97.00 (d, $^2J_{C-P}$ = 24.6 Hz, C_1), 70.23 (s, C_3), 16.68 (d, $^1J_{C-P}$ = 29.4 Hz, PMe_3). $^{31}P\{^1H\}$ NMR ($CDCl_3$, 161.92 MHz): δ −6.93. Anal. Calcd for $C_{12}H_{16}ClPPd$: C, 43.27; H, 4.84. Found: C, 43.19; H, 4.94.

Synthesis of IndPd($P(OMe)_3$)Cl (9). $P(OMe)_3$ (175 μL, 1.6 mmol) was syringed into a stirred Et_2O suspension (30 mL) of $\{(\eta^3\text{-Ind})Pd(\mu\text{-Cl})\}_2$ (**6**; 400 mg, 0.78 mmol) at room temperature. After it was stirred for 2 h, the resulting red solution was filtered and then concentrated to 15 mL. Addition of hexane (15 mL) resulted in the precipitation of an orange powder, which was filtered and washed with hexane to give an orange solid (460 mg, 82%). Recrystallization of a small portion of this solid from an ether solution at room temperature yielded crystals suitable for X-ray diffraction studies and elemental analysis. ^{1}H NMR ($CDCl_3$, 400 MHz): δ 7.24 (d, $^3J_{H-H}$ = 7.5 Hz, H_7), 7.10−7.06 (m, H_6 and H_4), 6.98 (t, $^3J_{H-H}$ = 7.5 Hz, H_5), 6.58−6.56 (m, H_2), 6.49 (d, $^3J_{H-H}$ = 16.8 Hz, H_1), 5.69 (d, $^3J_{H-H}$ = 2.3 Hz, H_3), 3.64 (d, $^3J_{H-P}$ = 12.9 Hz, $P(OMe)_3$). $^{13}C\{^1H\}$ NMR ($CDCl_3$, 100.56 MHz): δ 136.02 (d, $^3J_{C-P}$ = 7.4 Hz, C_{7a}), 134.56 (d, $^3J_{C-P}$ = 4.2 Hz, C_{3a}), 127.64 (s, C_6), 126.56 (s, C_5), 120.09 (s, C_7), 118.25 (s, C_4), 111.16 (d, $^2J_{C-P}$ = 10.6 Hz, C_2), 99.42 (d, $^2J_{C-P}$ = 34.95 Hz, C_1), 73.15 (d, $^2J_{C-P}$ = 7.05 Hz, C_3), 53.24 (s, $P(OMe)_3$). $^{31}P\{^1H\}$ NMR ($CDCl_3$, 161.92 MHz): δ 131.2. Anal. Calcd for $C_{12}H_{16}ClO_3PPd$: C, 37.82; H, 4.23. Found: C, 37.55; H, 4.29.

Synthesis of $[(\eta^1\text{-Ind})_2(t\text{-BuNC})_2Pd(\mu\text{-Cl})_2]$ (10). A stirred benzene solution (10 mL) of *t*-BuNC (161 μL, 1.44 mmol) was added to a stirred benzene solution (25 mL) of $\{(\eta^3\text{-Ind})Pd(\mu\text{-Cl})\}_2$ (**6**; 400 mg, 0.78 mmol) at room temperature. The resulting orange solution was stirred for 45 min, filtered, and evaporated to dryness. The residue was crystallized from Et_2O at 0 °C to give the product as orange crystals (300 mg, 57%). ^{1}H NMR ($CDCl_3$, 300 MHz): δ 7.89 (d, $^3J_{H-H}$ = 6.9 Hz, H_4), 7.38 (d,$^3J_{H-H}$ = 7.4 Hz, H_7), 7.13−7.02 (m, H_3, H_5, and H_6), 6.77 (d, $^3J_{H-H}$ = 5.01 Hz, H_2), 5.85 (br, H_1), 0.40 (s, *t*-BuNC-(CH_3)$_3$). $^{13}C\{^1H\}$ NMR (C_6D_6, 75.40 MHz): δ 153.55 (s, C_{7a}), 142.86 (s, C_{3a}), 141.06 (s, C_3 or C_5 or C_6), 125.75 (s, C_4), 125.25 (s, C_3 or C_5 or C_6), 125.18 (s, C_2), 124.34 (s, C_3 or C_5 or C_6), 121.39 (s, C_7), 57.07 (s, *C*Me$_3$), 44.11 (s, C_1), 28.90 (s, C*Me*$_3$). The missing resonance for CN is probably obscured under the residual solvent resonances at ca. 129 ppm. IR (KBr): 2204 cm^{-1} (s, CN). Anal. Calcd for $C_{28}H_{32}Cl_2P_2Pd_2$: C, 49.43; H, 4.74; N, 4.12. Found: C, 50.59; H, 4.90; N, 3.94. All our attempts to further purify this material were unsuccessful.

Calculation of the Energy Barrier to the Indenyl Rotation in Complexes 4, 7, and 9. The Holmes−Gutowski equation for a two-site exchange process involving molecular rotation, $\Delta G^{\ddagger}/RT_c = 22.96 + \ln(T_c/\delta\nu)$,[24] can be used to calculate the free energy of activation for the hindered indenyl rotation process. The two variables in this equation, the coalescence temperatures (T_c) and frequency differences ($\delta\nu$) for each pair of exchanging resonances, are listed below along with the

complex	exchanging protons	T_c (K)	$\delta\nu$ (Hz)	$\Delta G^{\ddagger}$ (kcal/mol)
4	H_1/H_3	368−373	824	16.2−16.5
	H_4/H_7	358−368	336	16.4−16.8
	H_5/H_6	348−358	76	16.9−17.4
7	H_1/H_3	358−363	409	16.2−16.5
	H_4/H_7	348−358	64	17.0−17.5
	H_5/H_6	318−328	29	16.1−16.5
9	H_1/H_3	358−368	344	16.4−16.8
	H_4/H_7	328−338	68	16.1−16.5
	H_5/H_6	318−328	28	16.1−16.9

corresponding calculated $\Delta G^{\ddagger}$ values. It should be noted that the temperatures at which the spectra were recorded were not calibrated and that the temperature increments studied were not sufficiently small to allow the determination of accurate coalescence temperatures. Nevertheless, these uncertainties are relatively insignificant and the average $\Delta G^{\ddagger}$ values thus obtained represent a reliable, qualitative estimate of the energy barrier to the indenyl rotation process.

Cyclic Voltammetry. Electrochemical measurements were performed on an Epsilon electrochemical analyzer using 0.002 M solutions of the palladium(II) complexes in a 0.1 M CH_3CN solution of *n*-Bu_4PF_6 (0.1 M). Cyclic voltammograms were obtained in a standard, one-compartment electrochemical cell using a graphite disk as the working electrode, a platinum wire as the counter electrode, and a silver wire as the reference electrode. The cyclic voltammetry experiments were performed in the potential range of −2.4 to 1.2 V using a scan rate of 100 mV/s. Under these conditions, the $E_{1/2}$ value for the Fc^+/Fc couple was 570 mV.

Acknowledgment. This work was made possible thanks to the financial support provided by the Natural Sciences and Engineering Reserach Council of Canada (operating grants to D.Z.) and Université de Montréal (scholarships to C.S.-S.). We are also indebted to Johnson Matthey for the generous loan of $PdCl_2$, to Drs. M. Simard, L. Groux, and F. Bélanger-Gariépy for their assistance with the X-ray analyses, and to Dr. Yaofeng Chen for his help in evaluating the catalytic activities of complexes **4** and **6** in the polymerization of ethylene. Prof. Boudjouk is thanked for supplying the experimental details for the reaction of 1-$SiMe_3$-Ind with $Na_2[PdCl_4]$.

Supporting Information Available: Complete details of the X-ray analysis of **4**−**7**, **9**, and **10**, including tables of crystal data, collection and refinement parameters, bond distances and angles, anisotropic thermal parameters, and hydrogen atom coordinates. This material is available free of charge via the Internet at http://pubs.acs.org.

OM034253N